

THE UNIVERSITY OF MICHIGAN
COLLEGE OF ENGINEERING
Department of Aerospace Engineering
High Altitude Engineering Laboratory

Technical Report

FUNDAMENTALS OF FOURIER
TRANSFORM SPECTROSCOPY

ucan
L. W. Chaney

ORA Project 05863

under contract with:

NATIONAL AERONAUTICS AND SPACE ADMINISTRATION

CONTRACT NO. NASr - 54(03)

WASHINGTON, D. C.

administered through

OFFICE OF RESEARCH ADMINISTRATION ANN ARBOR

February 1967

engm

UMR1133

Table of Contents

	Page
LIST OF FIGURES	v
FORWARD	vii
1.0 Introduction	1
2.0 History	3
3.0 Theory	6
3.1 The Michelson Interferometer	6
3.2 The Multiplex Advantage	10
3.3 The Throughput Advantage	11
3.4 Basic Concepts - The Fourier Transform Pair	15
3.5 Finite Mirror Drive - Apodizing - Scanning Function	16
3.6 Finite Solid Angle - Self Apodizing - Wavelength Shifting	19
3.7 Sampling - Aliasing - Periodic Ghosts - Random Jitter	21
3.8 Phase Errors - Electrical - Optical - Phase Compensation	27
3.9 Noise Theory	32
4.0 Data Handling	33
4.1 Digitizing	33
4.2 Computational Methods	34
5.0 Instrument	36
5.1 Classical Michelson - Slow Scan	36
5.2 Classical Michelson - Fast Scan	37
5.3 Skewed Michelson	37
5.4 Lamellar Gratings	38
5.5 Variations	39
6.0 Calibration	41
6.1 Wavelength	41
6.2 Sensitivity	42
6.3 Scanning Function	43
7.0 Summary	43
REFERENCES	45

FIGURES

		Page
1	Basic Interferometer	7
2	Typical Interferogram	9
3	Typical Spectra	9
4	Field of View Analysis	12
5	Fringe Field for γ_{\max} and L_{\max}	14
6	Fringe Field for $\gamma_{\max}/2$ and L_{\max}	14
7	Grating Fringe Field	14
8	Truncation Function	16
9	Scanning Function	17
10	Triangular Apodization	18
11	Self Apodizing Effects	21
12	Scanning Function vs. Frequency	22
13	Dirac Comb Scanning Function	25
14	Ghost Frequencies	27
15	PerCent Mean Error due to Time Jitter in Sampling	29
16	Digitizing Command and Interferogram Displacement	30
17	Phase Shift Plot	30
18	Asymmetrical Corrections	32
19	Skewed Michelson	37
20	Lamellar Gratings	38
21	Off-axis ray displacement	40

FORWARD

The following lecture on Fourier transform spectroscopy was prepared for a University of Michigan Engineering Summer Course in Precision Radiometry given June 27 to July 1, 1966.

The notes for the lecture are being reproduced here for those who might be considering the use of Fourier transform spectroscopy for the first time. The notes are brief but, hopefully, comprehensive enough to produce an awareness of the details which must be considered in order to obtain satisfactory results from the technique.

Descriptions of the technique by both Mertz¹ and Loewenstein² should be consulted for additional background and details. Also, recent articles by both Bell³ and Forman⁴ include tutorial presentations of the mathematical formulations, which are very instructive. Anyone interested in a more serious study is advised to consult J. Connes' thesis⁵ which is the most authoritative and complete study available.

Since the lecture was presented last summer several papers have appeared which demonstrate the power of the technique. The Connes have published the results of their astronomical observations of Mars and Venus.⁶ This data is truly amazing, and in the case of the Mars spectra, the resolving power of 1 cm^{-1} is 10 times better and the signal to noise ratio is 10 times higher than the best data obtained by classical techniques.

Bell³ has demonstrated the advantages of the technique in measuring the optical properties of solids. The complete Fourier transform gives not

only amplitude but, also, phase information. In the instrument described the samples to be studied are placed in one beam, and the change in amplitude as well as the phase rotation is measured. The extra phase information obtained is an important advantage of the method.

Dowling⁷ has reported high resolution results obtained in the far-infrared (80μ to 1000μ) using a lamellar grating interferometer with a theoretical resolution of 0.06 cm^{-1} . Spectra of CO, DCL, NO and H_2O have been obtained.

The University of Michigan, High Altitude Engineering Laboratory⁸ has reduced to spectra the data obtained from a high altitude balloon flight. Thermal radiation measurements with a resolution of 5 cm^{-1} from 500 cm^{-1} to 2000 cm^{-1} and an intensity accuracy of $\pm 1 \text{ erg sec}^{-1} \text{ cm}^{-2} \text{ sr}^{-1} / \text{cm}^{-1}$ were made. The measurements have been used to compute a vertical temperature profile which agrees very well with radiosonde profiles. A satellite version of this instrument is scheduled to be flown by Goddard Space Flight Center on a Nimbus satellite late in 1967 or early 1968.

1.0 INTRODUCTION

To introduce Fourier transform spectroscopy it seems appropriate to define the subject first. Mertz says in his new book Transformations in Optics¹, "Fourier transform spectroscopy is a disagreeable indirect way to measure a spectrum." Loewenstein says in his recent article, The History and Current Status of Fourier Transform Spectroscopy,² "Fourier transform spectroscopy is the technique of determining a spectrum by the Fourier transformation of an interferogram, which is the record produced by a two-beam interferometer as the path difference between the beams is varied from zero to some maximum value." Both of these definitions are valid. Mertz indicates some of the frustration that anyone who has worked in this field has been subject to; whereas, Loewenstein is quite precise.

It is certainly appropriate to ask, "Why bother with this technique, if it is so disagreeable?" The answer is short and simple; there are some measurements that cannot be made by any other technique. Some examples of measurements that fall into this category are far infrared, 10 cm^{-1} - 500 cm^{-1} , absorption studies, astronomical infrared spectroscopy, and night glow emission studies. Hence, the progress in Fourier transform spectroscopy since its revival in 1951 has been due primarily to workers in these fields. The first reduction of an interferogram to spectra was done by Fellgett⁹ who described the technique as multiplex spectroscopy and coined the term multiplex advantage which is now sometimes called the Fellgett advantage. The technique has also been called interference spectroscopy, but Fourier transform spectroscopy has become the accepted terminology.

Although the use of Fourier transform spectroscopy has been limited to the developers until now, this situation appears to be in the process of changing as it becomes commercially feasible to build a complete high resolution instrument. As of today, there are four companies manufacturing interferometers, two in the United States and two in England.

The first commercial interferometers were built by Block Associates based on the research work of L. Mertz. The original idea of this company was to build a low resolution, rapid scan instrument, the data from which could be reduced to spectra using commercially available wave analyser equipment. The applications for this instrument are engineering type rather than scientific type measurements. In spite of its limitations, the instrument has had relatively wide-spread use and has served to introduce a number of people to some of the intricacies of interferometry.

The other American manufacturer of interferometers is Idealab. Their designs have been inspired by the work performed for Vanasse and others at Air Force Cambridge Research Lab. Idealab is now offering an infrared instrument having 1 cm^{-1} resolution and a scanning time of 4 mm per second. Neither this instrument nor the Block instrument is at this time (Dec. 1966) complete in itself. A computer is required to complete the instrument, furnished by the users along with the interface. This procedure involves the user in the final design of the instrument.

Two English companies, Grubb Parsons, and Research and Industrial Instruments Company are now building far infrared instruments 10 cm^{-1} to 500 cm^{-1} . Both of these designs have been inspired by instruments built for Gebbie at the National Physical Laboratory.

The RIIC instrument is complete in that a computer is a part of the package. The user of the instrument has a spectra immediately after taking the data. Grubb Parsons offers its users a computer via Telex which is available to some of its English customers. These are the first complete instrument systems to be offered, and their application is limited to the far infrared but is indicative of future developments.

In spite of the fact that the superior energy gathering power of a Fourier transform spectrometer has been clearly established, the method has developed rather slowly due to the difficult computer interface. The difficulty is a two fold problem. One, the time required to make the transformation is quite long. Two, the difficulty of maintaining phase integrity tends to increase the computer time. Several groups are now working on these problems, and it seems that reasonable solutions are virtually at hand. We should, therefore, expect that Fourier transform spectroscopy will become much more wide-spread in the next few years.

A clear demonstration of the effectiveness of the method is the results recently reported by J. Connes and P. Connes.⁶ Using a Michelson interferometer at Kitt Peak, they obtained spectra of Venus in the 4.3μ CO_2 band with a resolution of approximately 1 cm^{-1} .

2.0 HISTORY

The general concept of Fourier transform spectroscopy was realized by many early workers such as Fizean, Michelson, Wood, and Ruben. A review of their efforts is given in a recent publication by Loewenstein,² who has done an excellent job in recounting the history of Fourier spectroscopy. However, it is appropriate to acknowledge the contributions of some of the

present day workers to the development of the technique.

The first modern worker in the field was Fellgett⁹ who recognized the multiplex advantage and converted the first interferogram to spectra. Shortly afterwards Jacquinet¹⁰ pointed out the throughput advantage of the interferometer, which coupled with the multiplex advantage inspired the work of Connes,¹¹ Strong, Vanasse, Gebbie¹², and Mertz.¹³ Madame Connes deserves a great deal of credit for her thesis⁵ published in 1961 covering all aspects of the subject. It is now available in an English translation and stands as an authority in the field. John Strong was an early contributor to the field with the development of the lamellar grating interferometer,¹⁴ but his greatest contribution has been in developing several graduate students who have made significant contributions. Gebbie, Mertz, and Vanasse have each made notable contributions and they have each inspired the development of commercial instrumentation. Mertz has been particularly influential by virtue of his position with Block Associates.

In the past few years contributions to the literature have come from many sources. A reflection of the developing interest was a symposium¹⁵ devoted exclusively to Fourier spectroscopy held in June 1965 at the Mellon Institute in Pittsburgh. Recent contributions have dealt with improved mathematical techniques for both taking the transform and correcting instrumental limitations. Finally, scientific measurements are now being reported which should lay to rest any doubts about the power of the method.

The High Altitude Engineering Laboratory, University of Michigan, under the sponsorship of Goddard Space Flight Center, NASA has been developing Fourier transform spectroscopy for the measurement of atmospheric

radiation. The initial measurements were made with a Block I-4 interferometer on a high altitude balloon in June 1963.

Subsequently, a much improved 5 cm^{-1} instrument was developed through a cooperative effort with G. S. F. C. The instrument was flown on a high altitude balloon on May 8, 1966. The optical parts of the instrument were designed primarily by University of Michigan personnel and the electronics by NASA personnel under the direction of Dr. R. A. Hanel.³¹

Dr. Hanel is Chief Scientist for the Laboratory for Atmospheric and Biological Sciences which is responsible for the development of the satellite version of the 5 cm^{-1} instrument. The satellite instrument is currently being built by Texas Instruments and is scheduled for flight on a Nimbus satellite late in 1967 or early 1968.

The further development of Fourier spectroscopy is currently being pursued by several laboratories and commercial organizations. Organizations known by the author to be so engaged are listed below.

Manufacturers:

Block Associates, 19 Blackstone St., Cambridge, Mass, 02139

Grubb Parsons Co., Walkergate, New Castly Upon Tyne 6,
England

Idealab, Box 228, Franklin, Mass., Tel. 617-528-9260

Research & Industrial Instruments Co., 17 Stannary St., London
S. E. 11, England

Texas Instruments, P. O. Box 6015, Dallas, Texas, 75222

Laboratories:

Aerospace Corp., Space Physics Laboratory, P. O. Box 95085,
Los Angeles, Calif., 90045, c/o J. M. Dowling

AFCRL, Optical Physics Laboratory, L. G. Hanscomb Field,
Bedford, Mass., 01730, c/o E. V. Loewenstein

Laboratories (cont'd):

Bell Telephone Laboratories, Inc., Murray Hill, N. J.,
c/o P. L. Richards

Center National De La Recherche Scientifique, Bellevue,
S & O, France, c/o J. & P. Connes

High Altitude Engineering Laboratory, University of Michigan
Ann Arbor, Michigan, 48105

Institute of Upper Atmosphere Physics, University of
Saskatchewan, Saskatoon, Canada, c/o G. G. Shepherd

Jet Propulsion Laboratory, Pasadena, California, c/o R. Beer

Laboratory of Molecular Spectroscopy and Infrared Studies, The
Ohio State University, Columbus, Ohio, 43210, c/o
E. E. Bell

McLennan Laboratory, Department of Physics, University of
Toronto, Toronto, Ontario, c/o H. P. Gustl

NASA, Goddard Space Flight Center, Laboratory for Atmos-
pheric and Biological Sciences, Greenbelt, Md., 20771,
c/o R. A. Hanel

National Environmental Satellite Center, ESSA, Washington,
D. C., c/o D. Q. Wark

National Physical Laboratory, Teddington, Middlesex, England,
c/o H. A. Gebbie

3.0 THEORY

The theory of Fourier transform spectroscopy has several aspects which can be discussed in various orders. The outline to be followed is given in the table of contents.

3.1 Introduction-The Michelson Interferometer

Although it is possible to apply Fourier transform methods to the Fabry-Perot and other multiple reflecting devices, this discussion will be limited to a Michelson two beam interferometer.

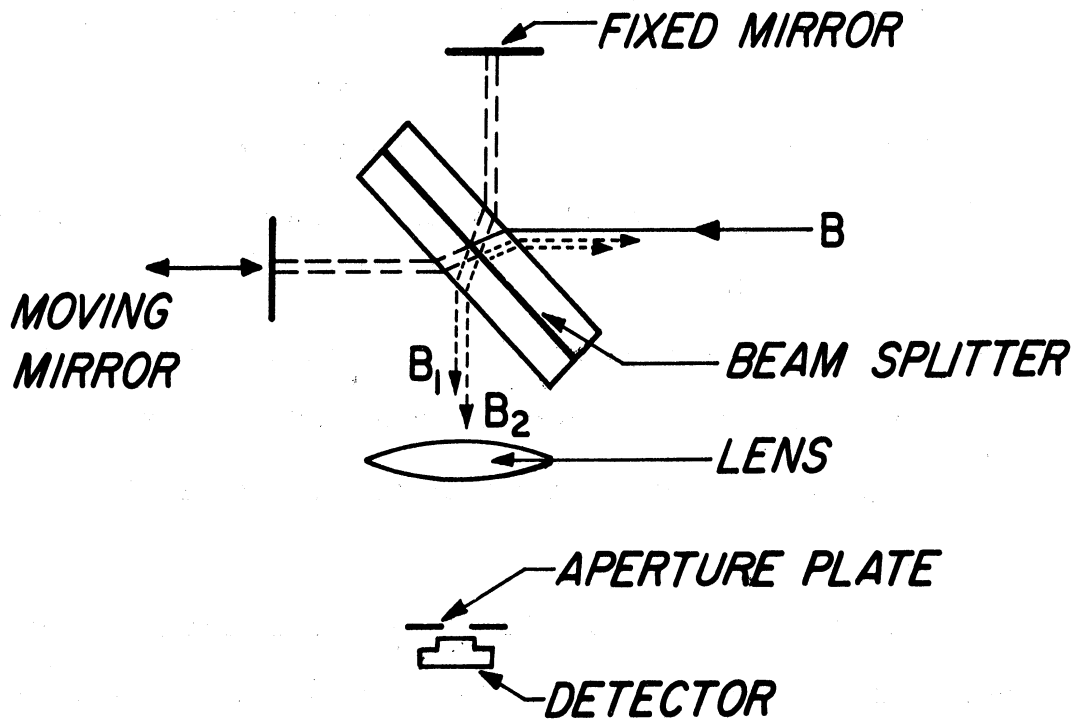


Fig. 1 Basic Instrument

An outline sketch of the basic instrument is given in Figure 1. The basic operation is as follows: The input radiation represented by the ray B is divided at the beam splitter into two rays B_1 and B_2 ; each ray is returned to the beam splitter and divided again. Two recombined beams are thus formed. One recombined beam is reflected back towards the input and lost while the other beam passes through the lens and is focused on the aperture plate and detector. The moving mirror is normally displaced through a distance $\pm L/2$ from a point of zero retardation such that the optical path difference is equal to $\pm L$.

- (1) The input radiation may be introduced at an angle of 30° to the beam splitter such that both recombined beams can be collected.^{17*}

- (2) The plane Michelson mirrors may be replaced by parabolic mirrors and a flat reflector at the focus to reduce the effect of mirror rotation. This type of mirror has been called a "cat's eye" by Connes⁶ and is used in his latest instrument.
- (3) The plane mirror may be replaced by corner reflectors for the same reason.¹⁸
- (4) The light paths may be folded by several auxiliary mirrors in such a way that the light is reflected from both faces of the moveable mirror. This has recently been described as the "Mobius Band"¹⁹ interferometer.

The purpose of the first modification is to collect more energy. The other modifications are made to minimize the signal loss due to any misalignment of the moveable mirror.

There are, of course, many possible variations in the mirror drive, beam splitter mount, and focusing optic. Some of these are discussed in the section on instruments.

The detector output as a function of optical path displacement is called an interferogram. A typical interferogram is shown in Figure 2 and the corresponding spectral distribution is given in Figure 3.

* Both beams are collected in the case of the skewed interferometer (see instruments).

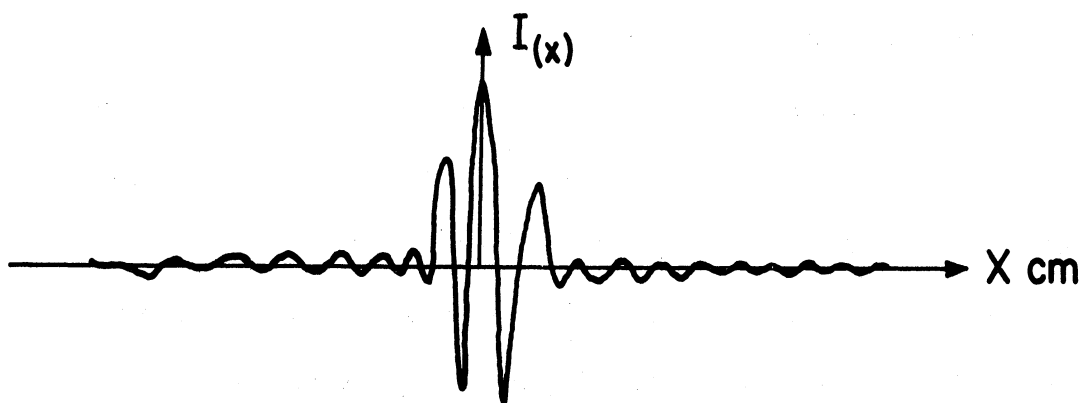


Fig. 2 Typical Interferogram

Under ideal conditions the interferogram is a completely symmetrical function, and normally only one half need be recorded. However, in most instruments there are phase shifts which produce asymmetries thus requiring the recording of both sides of the interferogram or necessitating the use of mathematical convolutions in the data processing.²¹

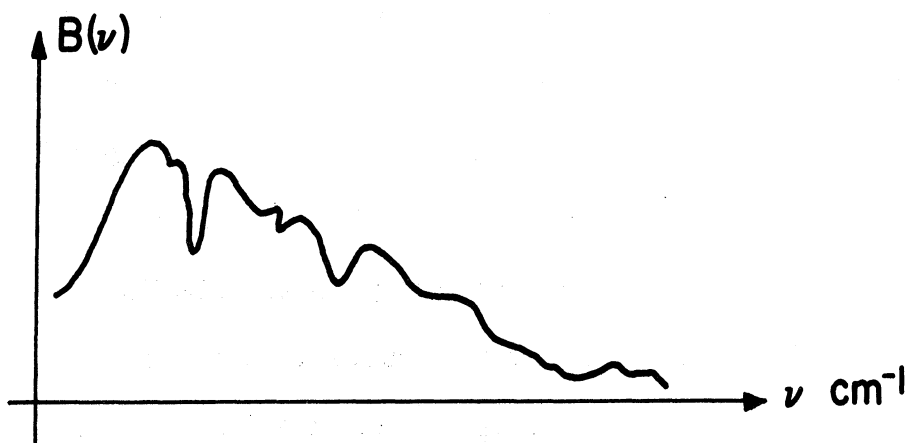


Fig. 3 Typical Spectra

3.2 The Multiplex Advantage

The multiplex or Fellgett advantage is the basic advantage that the interferometer has over conventional spectrometers and gave rise to the term "Multiplex spectroscopy"⁹ coined by Fellgett.

The basis of the advantage is that in observing a spectral element the increase in signal to noise ratio, S/N , is proportional to the square root of the elemental observation time T . If the different spectral elements are explored consecutively, as is done in a conventional spectrometer, the time available for each spectral element is $t = T/M$, where M is the number of spectral elements. The interferometer, however, observes all the spectral elements simultaneously for the total time T . Since the signal to noise is proportional to the square root of the observation time, then the gain $G = \sqrt{M}$, where M the number of resolution elements is exactly equal to the increase in observing time.

This advantage assumes that the noise is independent of the signal falling on the detector. The assumption is true for thermal detectors such as thermocouples and thermistor bolometers but not true for photon detectors. For this reason, the interferometer has found its greatest application in the infrared. The gain can be substantial if a wide spectral region is to be scanned. A typical value for M would be 400 which represents a signal increase of 20. The interferometer normally has two significant losses, half the energy is reflected back toward the source and almost half the remaining energy is lost in transmission through the beam splitter. Hence, we are left with a total gain of 5 over conventional instruments.

3.3 The Throughput Advantage

Before discussing the throughput advantage, throughput which has also been termed luminosity and etendue will be defined. The throughput of an optical instrument is a measure of the amount of light transmitted by an instrument having a given aperture and a given solid angle. The throughput can be expressed by

$$TP = \Phi/B \quad (1)$$

where Φ is the flux falling on the detector and B is the intensity of the source. In terms of the optical instrument

$$TP = A \Omega \tau \quad (2)$$

where A is the area of the aperture, Ω is the solid angle, and τ is the transmission factor and equation (1) is equal to equation (2). The transmission factor is actually the product of a number of factors but, in general, depends on the quality of the optical parts and would be one for a perfect instrument.

It is apparent that any increase in the solid angle will increase the throughput. However, for a spectrometer the permissible solid angle is limited since an increase in solid angle will decrease the spectral resolution. Thus, the product of the resolution R and the solid angle Ω is a constant. The advantage that the interferometer achieves is due to the fact that the product $R \Omega$ is much larger (two orders of magnitude) than in a grating spectrometer.

Interferometer	$R \Omega = 2 \pi$
Grating Spectrometer	$R \Omega = 0.07$

The derivation of the resolution solid angle product for the interferometer can be explained by referring to Figure 4.

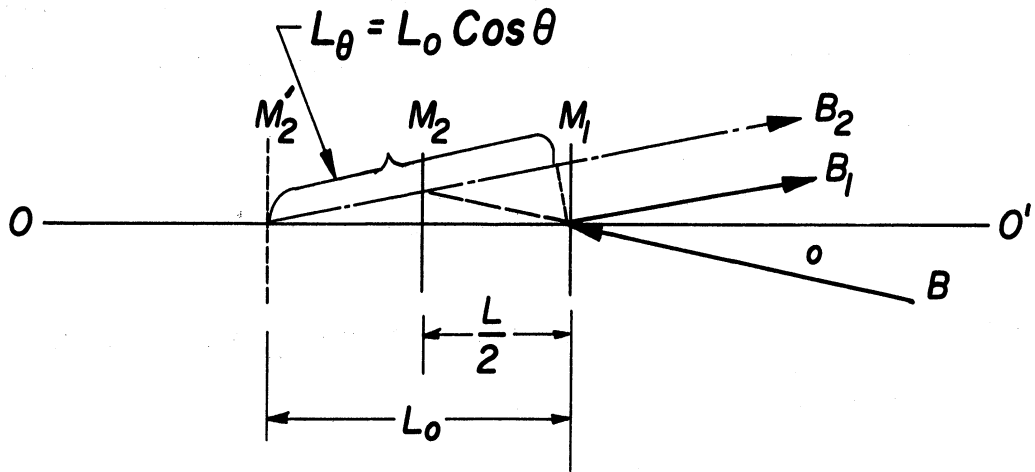


Fig. 4 Field of View Analysis

Line M_1 represents the fixed mirror, line M_2 the moveable mirror, and line M_2' the image of the moveable mirror. The distance $L/2$ is the maximum displacement of the moving mirror and L_0 is the maximum optical path difference along the optical axis OO' .

The input ray B enters the instrument at an angle which we define as the maximum acceptable angle. This ray is divided by the beam splitter into two equal and coherent components B_1 reflected from M_1 , and B_2 reflected from M_2 which appears to emanate from M_2' .

We are interested in the difference in path length for a ray along the axis compared with a ray entering at angle θ . Hence,

$$L_\theta = L_0 \cos \theta \quad (3)$$

$$\Delta L = L_0 - L_\theta = L_0 (1 - \cos \theta) = L_0 \frac{\theta^2}{2} \quad (4)$$

If we write this in terms of the solid angle corresponding to θ

$$\Delta L = L_0 \frac{\Omega}{2\pi} \quad (5)$$

It is now necessary to specify ΔL in terms of the wavelength of the input radiation. If ΔL is made equal to one wavelength of the shortest wavelength to be analyzed, the instrument will be optimized. In other words, the modulation drops to zero for the shortest wavelength at this point.

Substituting $\lambda = \Delta L$ in equation (5),

$$\lambda = L_0 \frac{\Omega}{2\pi} \quad (6)$$

The resolution of the interferometer is equal to the number of complete wavelengths contained in the maximum optical interference path length. Thus,

$$R = L_0 / \lambda \quad (7)$$

If this is substituted into (6), then

$$R \Omega = 2\pi \quad (8)$$

It is sometimes difficult to grasp why the interferometer is capable of accepting energy from such a large angle. The fundamental reasons are as follows:

(1) The instrument has rotational symmetry and makes use of a whole fringe: that is, the maximum space where the phase difference has a given value. This can be visualized with the aid of fringe diagram (see Figures 5, 6, and 7).



Fig. 5 Interferometer Fringe Field For ν_{\max} and L_{\max}

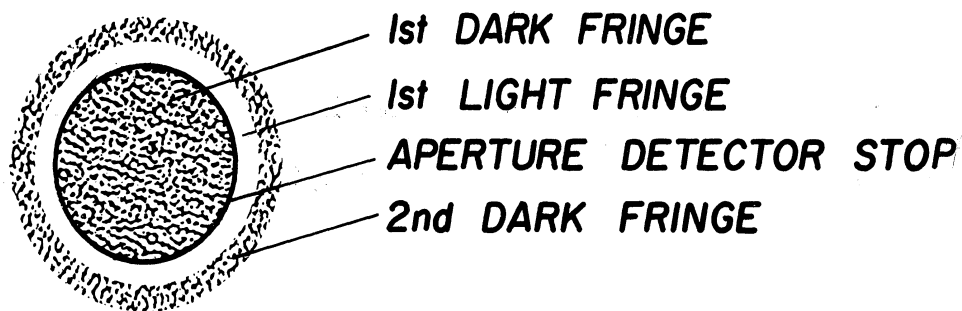


Fig. 6 Interferometer Fringe Field For $\nu_{\max}/2$ and L_{\max}

EXIT SLIT AND DETECTOR APERTURE

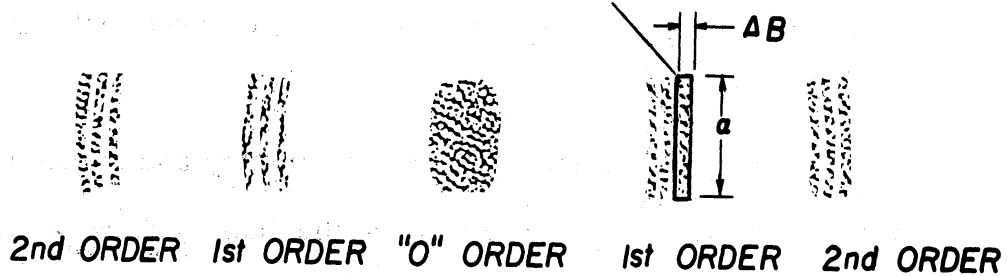


Fig. 7 Diffraction Grating Fringe Field

The fringes in the case of the spectrometer are not complete and the slit opening covers a very small portion of a total fringe. The slit has an angular height α and an angular width ΔB , the product of which is much smaller than the solid angle Ω for the interferometer.

(2) Jacquinot¹⁰ has shown that in addition to requiring circular symmetry, the input rays must be split by a transparent plate. This is a consequence of the fact that the observed fringe is the summation of many localized fringes which are created by rays spread across the entire aperture and aiming at various angles. The summation of rays over a large angular variation is possible because the variation of phase as a function of incidence angle is given by a second order term.

3.4 Basic Concepts

We have defined Fourier transform spectroscopy as the technique of determining a spectrum by the Fourier transformation of an interferogram which is the record produced by a two beam interferometer as the path difference between the beams is varied from zero to some maximum value.

Let $I(x)$ represent the amplitude of the interferogram record at some point (x) , and $B(\nu)$ represent the amplitude at a wave number ν . $I(x)$ and $B(\nu)$ are related by the Fourier transform and are written mathematically as a cosine Fourier transform pair where $B(\nu)$ is assumed to be an even function of ν .

$$I(x) = \int_{-\infty}^{+\infty} B(\nu) \cos 2\pi \nu x d\nu \quad (9)$$

$$B(\nu) = \int_{-\infty}^{+\infty} I(x) \cos 2\pi \nu x dx \quad (10)$$

These are the basic equations upon which Fourier transform spectroscopy is based. There are, however, limitations. The first obvious one is that the limits of integration are improper. The equation, as written, implies that the length of the mirror drive is infinite, which is, of course, impossible.

3.5 Finite Mirror Drive

In the case of a real interferometer, the interferogram is recorded for a finite length of mirror travel. The maximum distance from a position of zero retardation we call L . Thus, equation (10) becomes

$$B'(\nu) = \int_{-L}^{+L} I(x) \cos 2\pi \nu x dx \quad (11)$$

This is a truncated cosine function and, in general, $B'(\nu)$ will be different from the observed spectra $B(\nu)$.

$B'(\nu)$, however, can be written as the convolution of $B(\nu)$ and a scanning function $t(\nu)$ which is defined in the following way.

Let $T(x)$ a truncation function be defined in the following way:

$$T(x) = 1 \quad -L \leq x \leq +L \quad (12)$$

$$T(x) = 0 \quad \text{otherwise.} \quad (13)$$

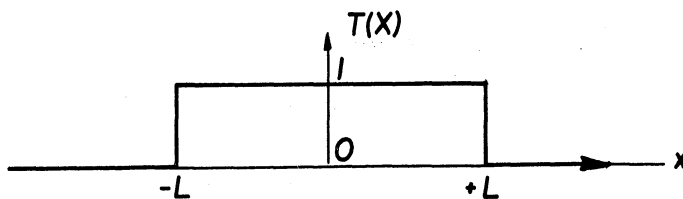


Fig. 8 Truncation Function

Hence, we can write

$$B'(v) = \int_{-\infty}^{+\infty} T(x) I(x) \cos 2 \pi v x dx \quad (14)$$

From the theory of Fourier transforms the convolution theorem says that the Fourier transform of the product of two functions is equal to the convolution of the Fourier transforms of the two functions.

If we denote the Fourier transform of $T(x)$ by $t(v)$, then we can express equation (14) as

$$B'(v) = t(v) * B(v) \quad (15)$$

The Fourier transform of $T(x)$ is

$$t(v) = 2 L \sin \frac{2 \pi L v}{2 \pi L v} \quad (16)$$

and is called the scanning function.

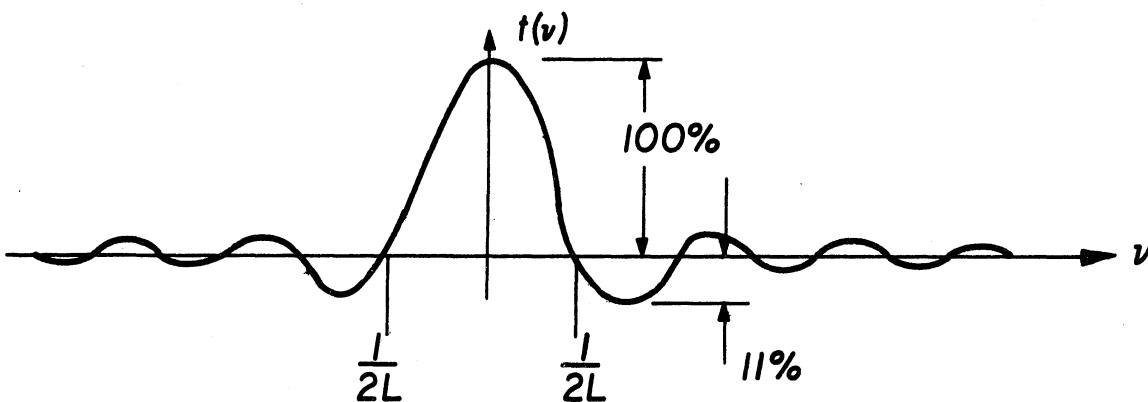


Fig. 9 Scanning Function

This particular scanning function is undesirable since the first side lobes are equal to 11% of the main lobe thus producing false perturbations in the resolved spectrum. The effect is particularly pronounced in the case of emission spectra. The scanning function can be easily modified by altering the truncation function $T(x)$.

Any alteration of the truncation is termed apodizing and is analogous to shaping the slits in a conventional spectrometer. The most commonly used apodizing function is a triangular function which produces a $(\sin x/x)^2$ scanning function (see Figure 10). This particular

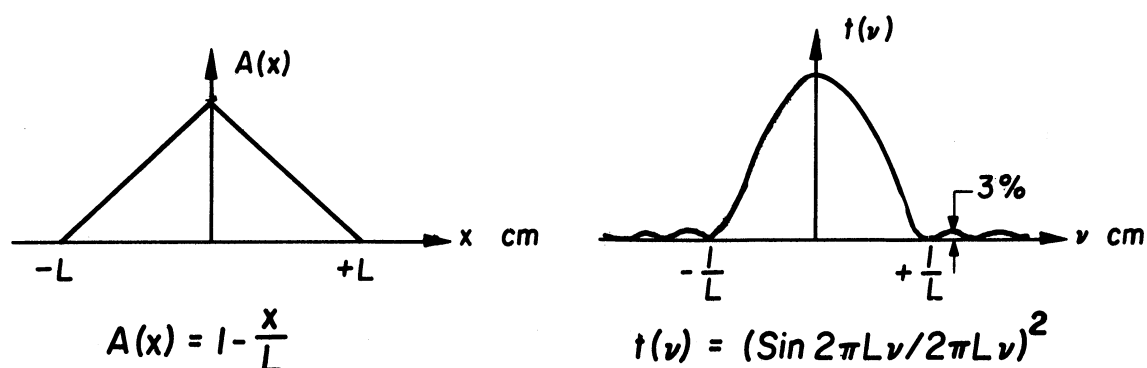


Fig. 10 Triangular Apodization

function is widely used and easy to apply; all the secondary lobes are positive, and it is identical to a grating spectrometer with rectangular slits. This represents, however, a rather severe apodization in that it reduces the resolution by a factor of two. The Connes' have used an apodizing function⁵ such that

$$A(x) = \left[1 - \left(\frac{x}{L} \right)^2 \right]^2 \quad (17)$$

Many others have been proposed, such as

$$A(x) = \cos \frac{\pi x}{2L} \quad (18)$$

Both of these functions tend to preserve the peak of the interferogram which contains most of the information while attenuating the wings more sharply. Essentially, the exact form of the apodizing function is a matter of choice of the experimenter depending on his instrument and the spectrum to be resolved.

With the introduction of the apodizing function, the new equation which expresses the convolved spectra becomes

$$B'(\nu) = \int_{-\infty}^{+\infty} T(x) A(x) I(x) \cos 2\pi \nu x dx \quad (19)$$

and can be rewritten:

$$B'(\nu) = 2 \int_0^L A(x) I(x) \cos 2\pi \nu x dx \quad (20)$$

3.6 Finite Solid Angle

The limitation on the solid angle was mentioned under the section on Throughput advantage. The path difference for the rays along the optical axis are longer than those along the periphery. The effect of this variation in path length is two-fold.

(1) The amplitude of the interferogram is attenuated as the path length increases.

(2) The number of wavelengths of the input radiation for a given axial path difference is decreased.

The first effect is known as self-apodization and it can be shown that that function has the following form:

$$\psi(\nu, x) = \frac{\sin \pi \nu x \frac{\Omega}{2\pi}}{\pi \nu x \frac{\Omega}{2\pi}} \quad (21)$$

This function is similar to any other apodization function except that it is also a function of frequency.

The other effect on the interferogram is to modify the frequency ν such that

$$\nu' = \nu \left(1 - \frac{\Omega}{4\pi} \right) \quad (22)$$

Hence, the new expression for the recorded interferogram is:

$$I(x) = \int_{-\infty}^{+\infty} B(\nu) \frac{\sin \pi \nu x \frac{\Omega}{2\pi}}{\pi \nu x \frac{\Omega}{2\pi}} \cos 2\pi x \nu \left(1 - \frac{\Omega}{4\pi} \right) d\nu \quad (23)$$

The effect of self apodization can be seen quite clearly by comparing two interferograms of monochromatic radiation both with and without self apodization.

Since the self apodizing function is also a function of frequency as well as

displacement, the new scanning function will also be frequency sensitive (see Figure 11).

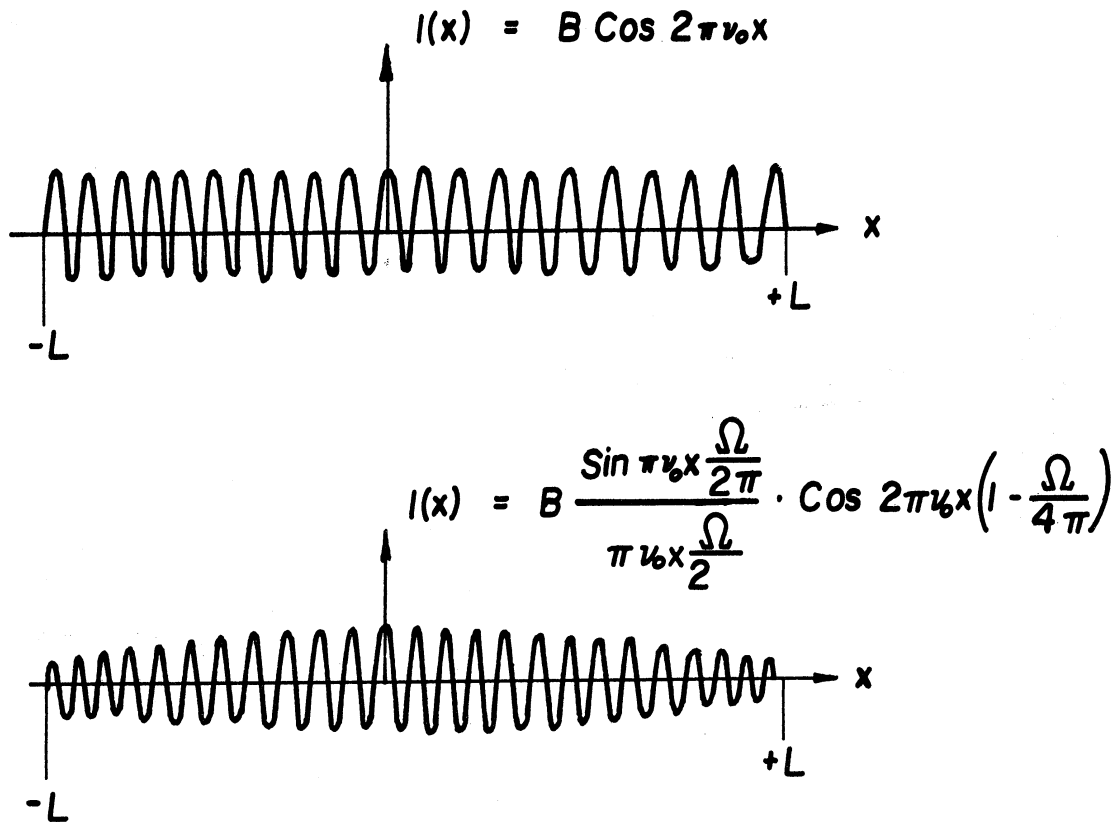


Fig. 11 Self Apodizing Effects

The variations in the scanning function for an interferometer* are given in Figure 12**. The broadening of the function with increased frequency can be clearly noted.

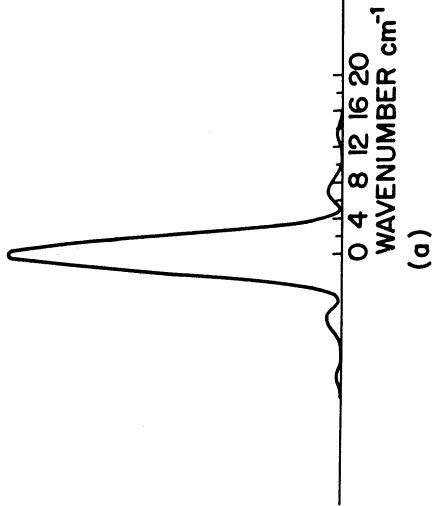
3.7 Sampling

Up to this point we have been considering the interferograms as continuous functions with no regard to how the transformation is to be made.

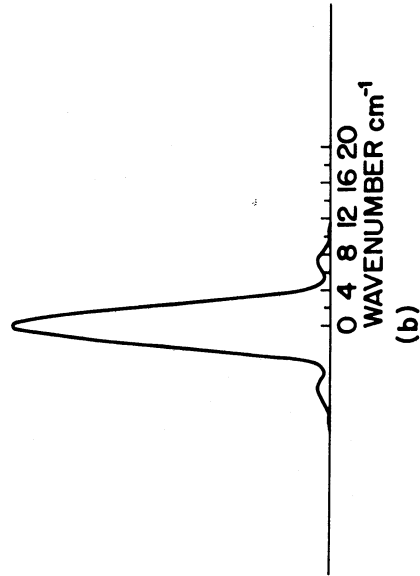
* Interferometer developed by High Altitude Laboratory

** This work was done by Surh and has not been published yet.

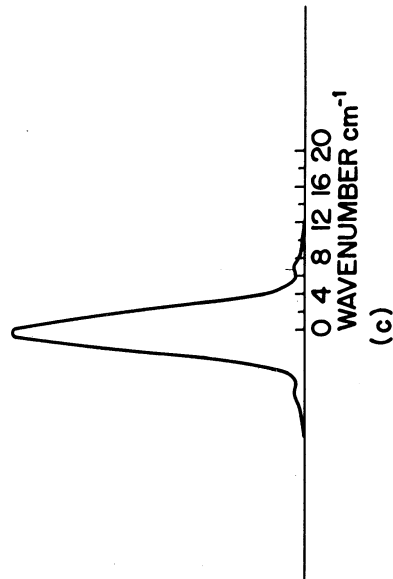
INSTRUMENT FUNCTION
AT 500 cm^{-1}



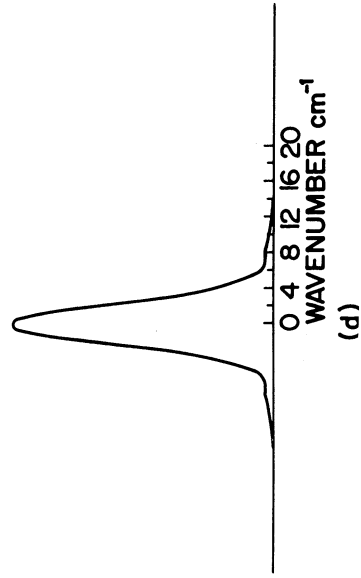
INSTRUMENT FUNCTION
AT 1000 cm^{-1}



INSTRUMENT FUNCTION
AT 1500 cm^{-1}



INSTRUMENT FUNCTION
AT 2000 cm^{-1}



INSTRUMENT FUNCTION
AT 2500 cm^{-1}

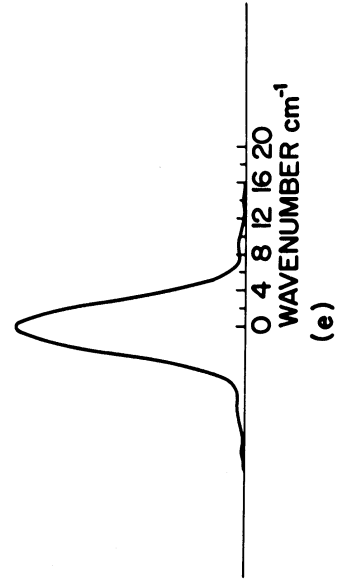


Fig. 12 Scanning Function vs. Frequency

Although a great deal of thought and effort have gone into the construction of various analogue devices for performing the transformation, the only satisfactory technique is to digitize the interferogram for processing on a digital computer. This process, itself, creates some problems and raises some questions which must be answered.

The questions are:

- (1) How often should we sample?
- (2) What are the modifications of scanning function?
- (3) Are spurious frequencies generated?
- (4) What is the effect of inaccurate sampling?

These questions have been encountered by communication engineers and their solutions can be applied to this situation.

Consider the first question; the sampling theorem tells us that all the information contained in the function $I(x)$ with a maximum spectral frequency (ν_{\max}) can be described completely by a finite number of sampled data $I(nh)$. The sampling interval, h , is given by $\frac{1}{2} \nu_{\max}$. This criterion for determining the value of h was followed in the initial design of our interferometer, but it was found that the noise at the high frequency end of the spectrum could be reduced by decreasing h . As a result of empirical testing, a value of $h = \frac{1}{4} \nu_{\max}$ was chosen. By using the shorter sampling interval, the digitizing noise in the spectrum was reduced to one per cent of full scale.

The selection of the sampling interval also affects the scanning function. The act of sampling is equivalent to multiplying the interferogram by a periodic Dirac comb function. The Dirac comb is given by:

$$R_h(x) = h \sum_{-\infty}^{+\infty} d(x - nh) \quad (24)$$

where h is the sample spacing and n is the sample number. This function has the effect of modifying the apodizing function; hence, we can write a new apodizing function which is the product of $A(x)$ and $R_h(x)$. The Fourier transform of the product is

$$P(\nu) = \sum_{-\infty}^{+\infty} d\left(\nu - \frac{n}{h}\right) \quad (25)$$

and is, except for a factor of $1/h$, another Dirac comb function with a frequency distribution equal to $1/h$. If the spectrum is defined by the equation

$$B(\nu) = \int_{-\infty}^{+\infty} I(x) \cos 2\pi \nu x dx \quad (26)$$

then the new resolved spectrum will be:

$$B'(\nu) = B(\nu) * P(\nu) = B(\nu) * \sum_{-\infty}^{+\infty} d\left(\nu - \frac{n}{h}\right) \quad (27)$$

The new scanning function defined by the Dirac comb is actually a series of scanning functions spaced at frequency intervals equal to $1/h$. It is very important that contributions to the spectrum be limited to the main region of interest; otherwise, unwanted contributions will be received as one of the other scanning functions scans the adjacent spectrum.

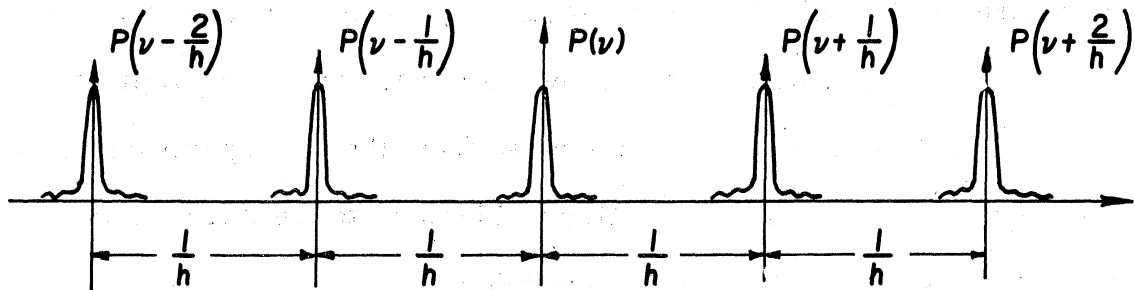


Fig. 13 Dirac Comb Scanning Function

It can also be seen that if the criterion is to have $h = \frac{1}{2} \nu_{\max}$ then, ideally, there should be no overlap. There are, however, two practical considerations that require that $1/h$ be increased: (1) the spectral cut-off of the instrument cannot be made perfectly sharp, and (2) the sampling interval cannot be made perfect. There is always a given amount of "jitter" in the length of the interval.

The statement is often made in the literature that the number of points computed in the spectrum should be equal to the number of points sampled in the interferogram. This statement is based on using a sampling interval equal to $\frac{1}{2} \nu_{\max}$. In practice, approximately half as many spectrum points may be computed as interferogram samples based on a one sided interferogram. If a double sided interferogram is used then the interferogram points will be doubled again. Hence, in practice there may be more than four times as many interferogram points as spectrum points calculated.

The last two questions regarding sampling will have to be considered

together. Any variation in the sampling interval either periodic or random will introduce errors in the computed spectra. Modulation of the sampling interval creates "ghosts" in spectroscopic terminology or side band frequencies in communication terminology. Furthermore, the power that manifests itself as false signals is derived from the true spectrum and hence, the true spectrum is attenuated. This is identical to the situation that exists in the case of a frequency modulated carrier.

Connes⁵ considered this problem for the case of monochromatic radiation and the modulation of the mirror drive in a sinusoidal fashion.

If we let x = the optical path displacement, then

$$x = Vt + \epsilon \sin (2 \pi t / \theta) \quad (28)$$

where V is the velocity of the mirror, t time, and θ is the period of the velocity modulation. The interferogram function can now be written as a function of t such that

$$\begin{aligned} I(t) &= B(\nu_0) \cos 2\pi \nu_0 \left[Vt + \epsilon \sin (2\pi t / \theta) \right] \\ &= B(\nu_0) \cos (\Omega_0 t + \beta \sin \omega t) \end{aligned} \quad (29)$$

where Ω_0 is the carrier frequency and β is the modulation index. Thus, one is led to the classical problem of studying the spectrum of a frequency modulated sine wave. A graphical representation of equation (29) is shown in Figure 14.

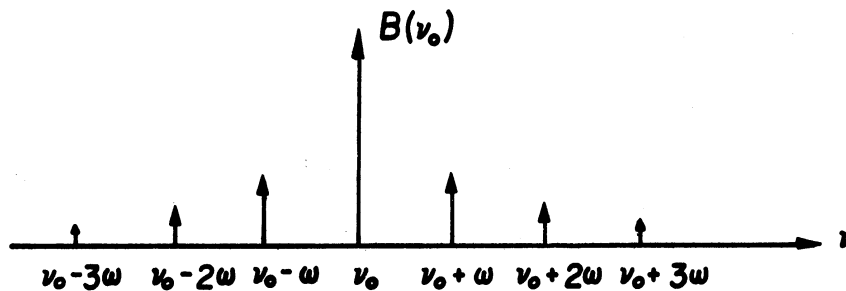


Fig. 14 Ghost Frequencies

The simplified case just illustrated does not exist in practice. The carrier is the spectral band of frequencies, $\Delta \nu$, to be analyzed, and except in special cases the modulation will be random in amplitude and frequency distribution.

The general case of the random modulation of a spectral frequency band was studied by M. Surh²⁰. The result of this study was the development of a technique for predicting the error in the resolved spectrum resulting from "jitter" in the sampling interval. The curves given in Figure 15 can be used to determine the spectral error due to a given maximum sampling jitter. As might be expected, "jitter" in the sampling period produces the largest errors at the shortest wavelengths.

3.8 Phase Errors

Phase errors are those errors which destroy the basic symmetry of the interferogram. These errors are created by three distinct mechanisms.

(1) Lack of symmetry in the optical path. A normal beam splitter is basically an asymmetric device since the beam splitting coating is on one side of the substrate. The beam splitter would have to be made like a sandwich with a substrate on both sides of the coating in order for the paths to

be symmetrical. Any distortions in either the beam splitter or the Michelson mirrors will also contribute to the asymmetry.

(2) Electrical phase shifts in the amplifiers.

(3) Displacement between the digitizing command and the interferogram function (see Figure 16).

The errors arising from the lack of symmetry in the optical path are, in general, non-linear functions of frequency, but the magnitude is only a few degrees; whereas, the errors of the third type are strictly linear functions of frequency. The electrical phase shifts are a combination of both linear and non-linear frequency functions and cannot be distinguished in analyzing the interferogram.

It can be seen from Figure 17 that any lack of synchronization between the digitizing command and the interferogram will cause severe problems, and perfect synchronization is also impossible to maintain. A number of people have considered this problem and it is still being pursued. Connes originally proposed the calculation of both the sine and cosine terms such that $B(\nu) = \sqrt{C^2 + S^2}$. This method has several disadvantages:

(1) The computation is increased.

(2) The scan must be made both positive and negative from zero retardation.

(3) The signal to noise ratio is increased.

The essential elements of the technique^{21, 22} which has been developed to handle this problem is as follows. Since the phase function is a continuous function, it can be determined from the interferogram calculated at a very low resolution. This is done by first calculating a low resolution spectrum

α = The maximum change in the length of a sampling period.
Nominal sampling period = 1.0

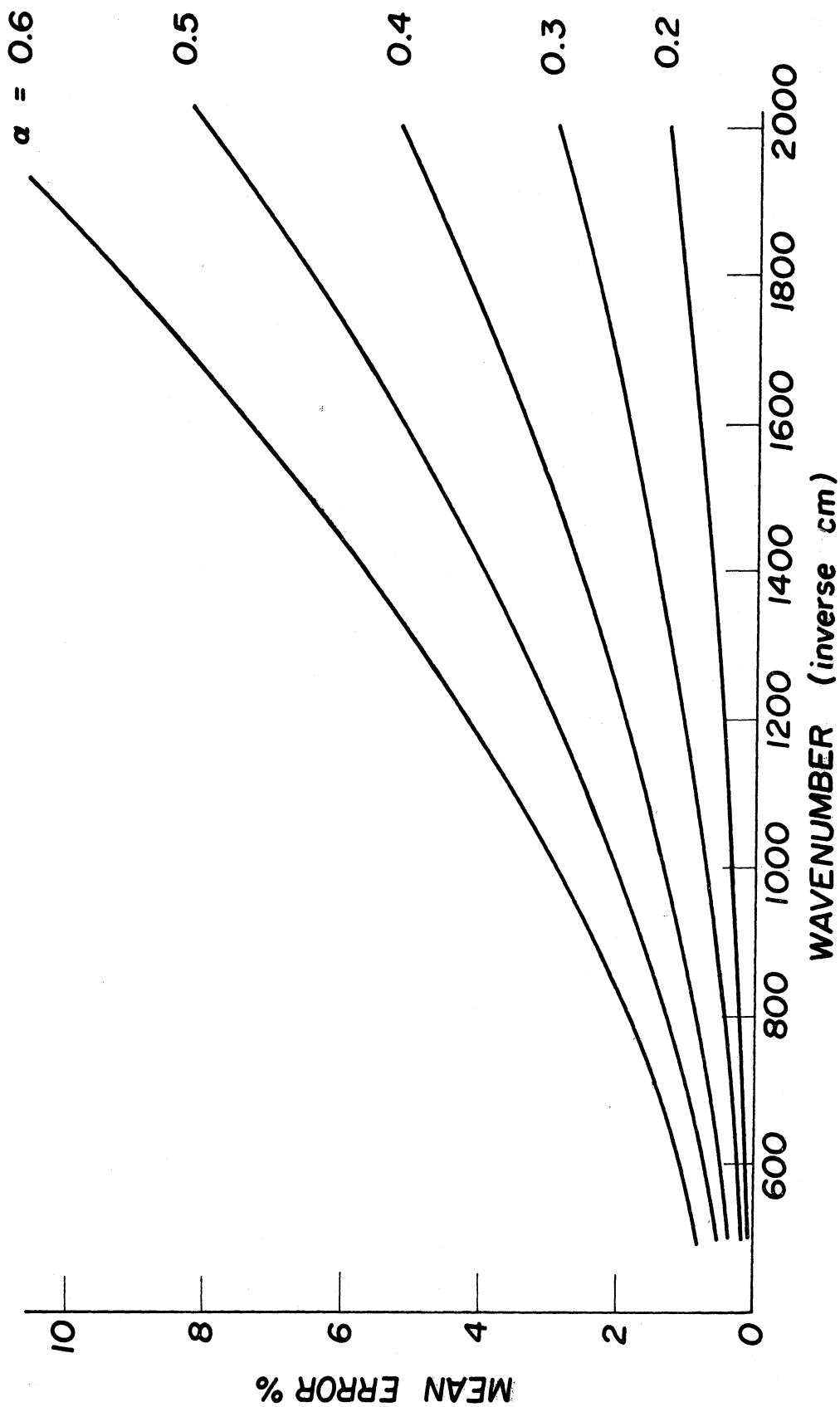


Fig. 15 Per Cent Mean Error Due to Time Jitter in Sampling

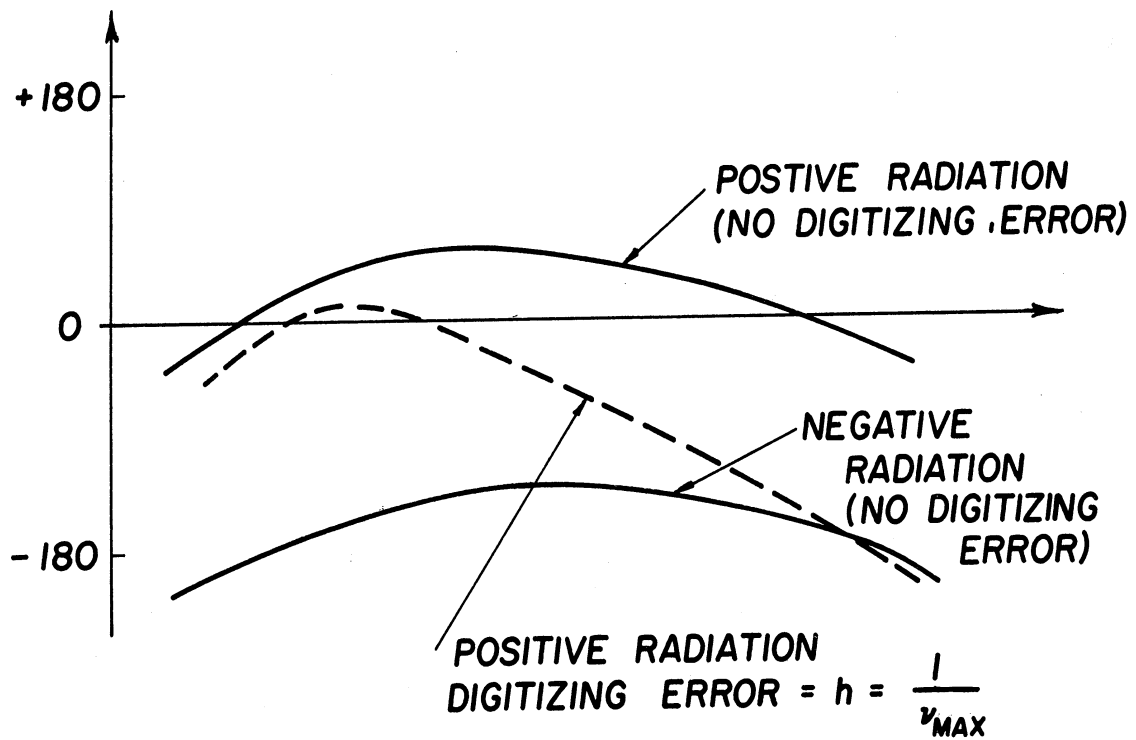


Fig. 16 Digitizing Command and Interferogram Displacement

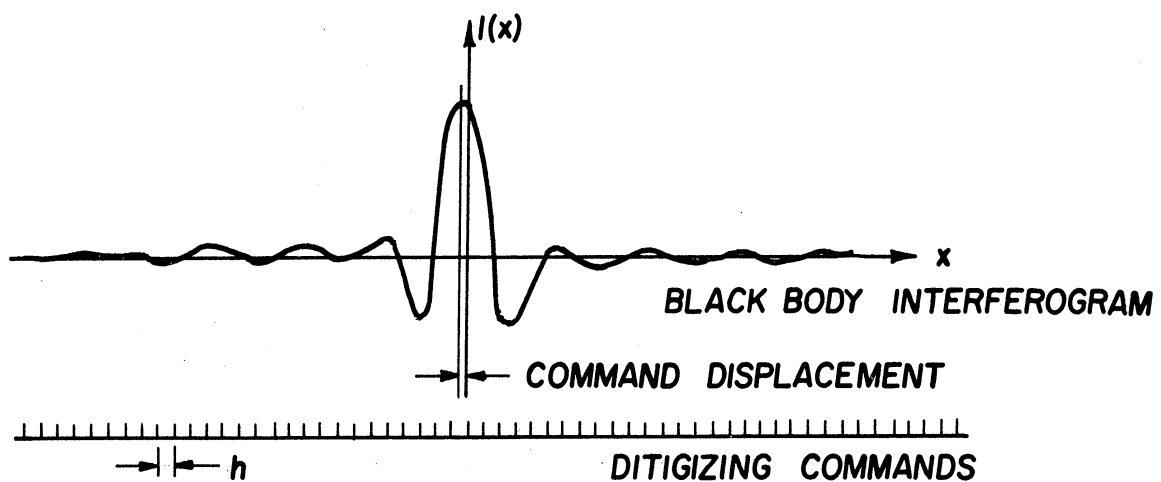


Fig. 17 Phase Shift Plot

using a few points around zero retardation.

$$B'(\nu) = \left\{ \left[2 \int_0^{L/F} A(x) I(x) \cos 2 \pi \nu x dx \right]^2 + \left[2 \int_0^{L/F} A(x) I(x) \sin 2 \pi \nu x dx \right]^2 \right\}^{1/2} \quad (30)$$

where F , is that fraction of the interferogram used for the calculation. The phase information is then used to construct a new function $Q(x, \phi)$ which is convolved with the asymmetrical interferogram $I(x)$. Thus,

$$I(x) * Q(x, \phi) = I'(x) \quad (31)$$

where $I'(x)$ is a symmetrical function. Now $B'(\nu)$ can be computed by

$$B'(\nu) = 2 \int_0^L A(x) I'(x) \cos 2 \pi \nu x dx \quad (32)$$

In applying this method there must be a prominent feature on the interferogram from which to start the calculations; this is nearly always the case.

$$B''(\nu) = \left\{ \left[2 \int_0^{L/F} A(x) I(x) \cos 2\pi\nu x dx \right]^2 + \left[2 \int_0^{L/F} A(x) I(x) \sin 2\pi\nu x dx \right]^2 \right\}^{1/2}$$

$$I(x) * Q(x, \phi) = I'(x)$$

$$B'(\nu) = 2 \int_0^L A(x) I'(x) \cos 2\pi\nu x dx$$

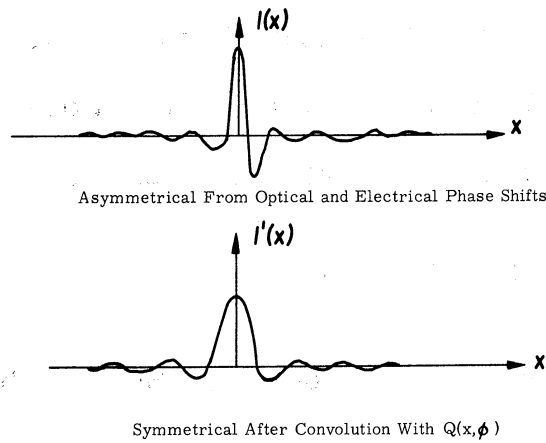


Fig. 18 Asymmetrical Corrections

3.9 Noise Theory

When noise is present in the interferogram, the computed spectra

$B'(\nu)$ is

$$\begin{aligned} B'(\nu) &= 2 \int_0^L A(x) \left[I(x) + n(x) \right] \cos 2\pi\nu x dx \\ &= 2 \int_0^L A(x) I(x) \cos 2\pi\nu x dx + 2 \int_0^L A(x) n(x) \cos 2\pi\nu x dx \\ &= P(\nu) * B(\nu) + P(\nu) * N(\nu) \end{aligned} \quad (33)$$

where $n(x)$ is the noise and $N(\nu)$ is the Fourier transform of $n(x)$.

If the noise is white noise in the interferogram and uncorrelated with the signal, then it will be white noise in the spectrum. Madame Connes made an extensive study of noise and signal to noise. An important conclusion of this work is that the cosine transform gives a better S/N ratio than the complete transform. Once this has been pointed out, it is rather obvious that a noise term arises from both the sine and the cosine and add in the same way as the signal. Since both noise terms are equal in magnitude, the total noise will be increased by $\sqrt{2}$.

We have already discussed the noise which arises due to "jitter" in the sampling interval. The other sources of noise are not peculiar to the interferometer. Specifically, reference is made to various types of interference both electrical and mechanical, digitizing noise from the A-D conversion, and amplifier saturation. Special care should be exercised in handling the signal to avoid saturation effects. In many instruments a dynamic range of 2000 to 1 must be provided.

4.0 DATA HANDLING

4.1 Digitizing

Let us assume that we have an interferometer which is capable of producing an interferogram such that

$$B(\nu) = 2 \int_0^L A(x) I'(x) \cos 2\pi \nu x dx \quad (34)$$

where $I'(x)$ is a symmetrical interferogram which includes the self-apodizing and the noise components. For computational purposes, it can be written

$$B'(\nu) = 2h \sum_0^N A(nh) I(nh) \cos 2\pi\nu nh \left(1 - \frac{\Omega}{4\pi} \right) \quad (35)$$

where h is the sampling interval and n is the sample number.

In order to carry out the computation, it is necessary that the amplitude of $I(n, h)$ be measured at intervals corresponding to h . There are two standard techniques for accomplishing the process. The Moire fringe technique used by far infrared workers has the advantage that the spacing can be made some integral number of microns. The other technique is to use a monochromatic source and an auxiliary detector. The monochromatic radiation is, of course, modulated by the same Michelson mirrors that modulate the measured radiation. The signal produced at the auxiliary detector will be a sine wave extending from $-L$ to $+L$. The sine wave is squared and used to trigger an A-D converter, a basic part of the instrumentation. The output of the A-D converter is the basic digital information which must be used to compute the transform. This information must be stored by some suitable means for processing by a digital computer. There are many techniques presently available for the storage and handling of the digital information such as magnetic tape, core storage, punched paper tapes, and punched cards. This type of equipment is in a continuous state of development and if additional information is required the appropriate manufacturers should be consulted.

4.2 Computational Methods

There has been considerable progress in computational methods in the last five years, which has aided tremendously in the development of the Fourier transform method.

A typical interferogram may be sampled at 1000 points, and values of $B'(v)$ computed at 1000 points. Then, for each value of v , there are 1000 values of nh and 1000 cosines corresponding to each nh to be computed. Altogether for this typical case there would be 1000 x 1000 values of cosines to be computed. The University of Michigan IBM 7090 requires an average of 0.47 mil-sec to compute a cosine to an accuracy of 7 places. Thus, 8 minutes of computer time would be required for one interferogram.

Thus, a formidable amount of time could be required for a modest experiment. In fact, the required computer time was a serious limitation on the development of the technique for weather satellite applications.

In order to reduce the computer time required, various recursion formulae were investigated. J. Connes⁵ proposed the use of the recursion formula of Tchebieheff

$$\cos (p + 1) x = 2 \cos x \cos px - \cos (p - 1) x$$

This particular recursion formula reduced the computer time to 1.5 minutes.

Later, a faster method proposed by Billings²³ was used. A new variable t is introduced, defined as follows:

$$t_{n+2} = 0$$

$$t_{n+1} = 0$$

$$t_n = A(nh) I(nh)$$

$$t_k = t_{k+1} (2 \cos 2 \pi \nu kh) - t_{k+2} + A(kh) I(kh)$$

With these expressions $B'(\nu)$ is

$$B'(\nu) = h \sum_0^N A(kh) I(kh) \cos 2 \pi \nu kh = h (t_1 - t_2 \cos 2 \pi \nu h) \quad (37)$$

This method reduced the computing time to 40 seconds and was used extensively by the University of Michigan.

However, the latest method²⁴ described by Cooley and Tukey has reduced the time to 14 seconds and is now being adopted by most workers in this field. An IBM 7094 computer is capable of performing the same transformation in 3 seconds using the Cooley-Tukey method. The interferometer designed for weather satellite application has a scan time of 10 seconds which permits real time reduction of spectra.

The introduction of the Cooley-Tukey method is a significant landmark in the development of Fourier spectroscopy and should lead to its more rapid future growth.

5.0 INSTRUMENTS

Several types of Fourier spectrometers are described in reasonable detail in the literature.^{3, 6, 25, 26, 27} Rather than duplicate the descriptions of the individual instruments, the instruments have been grouped into categories and the distinctive features of each category have been noted.

5.1 Classical Michelson - Slow Scan

The principal feature of this group is that the Michelson mirrors are orthogonal, producing one exit beam. Furthermore, the moving mirror is mounted on a lapped slide and driven by means of a fine screw through some intermediate coupling to eliminate modulation effects. The position

of the mirror is determined either by counting fringes from a monochromatic source or from a Moire grating. An instrument of this type is described by Gebbie,²⁵ and good examples are manufactured by Grubb-Parsons, RIIC and Idealab.

5.2 Classical Michelson - Fast Scan

The basic difference between the fast and slow scan instruments is in the mirror drive. The moving mirror instead of being mounted on a precision slide is mounted on parallel springs. This system works quite well for short scans. Gebbie²⁵ reported a mirror rotation of only one arc second for a travel of one centimeter. This is both the most accurate and the longest travel reported for this type of drive. The instrument described uses a micrometer screw for the drive, whereas others, such as the Block instruments and the High Altitude Engineering instrument, use a coil in a permanent magnet field.

5.3 Skewed Michelson^{6, 26}

The principal modification of this instrument is to alter the position of the Michelson mirrors from their orthogonal position.

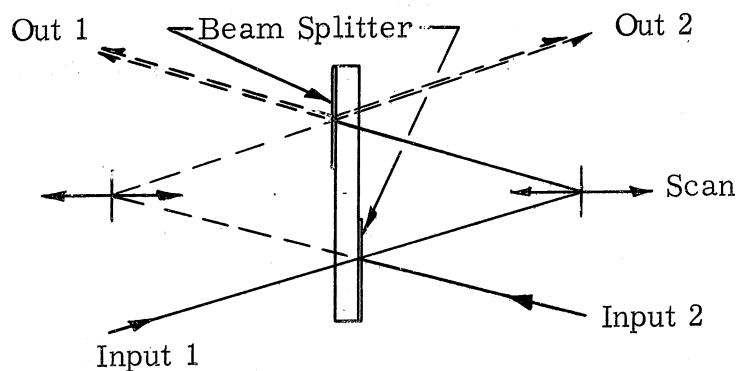


Fig. 19 Skewed Michelson

There are several advantages to this system

- (1) The optical paths are completely symmetrical.
- (2) Two inputs are available which can be extremely useful for planetary spectroscopy.
- (3) The two outputs can be combined to increase the signal to noise ratio.

The principal disadvantage of this arrangement is that it is less compact than the conventional Michelson. The beam splitter occupies twice the normal area and the field of view is restricted by the longer optical paths.

5.4 Lamellar Gratings^{7, 14, 28, 29}

The lamellar grating instrument was designed for use in the far infrared ($100\mu - 1000\mu$) to circumvent the beam splitter requirement. The Michelson mirrors are replaced by the lamellar gratings which are arranged so that one set is fixed and one set is moveable.

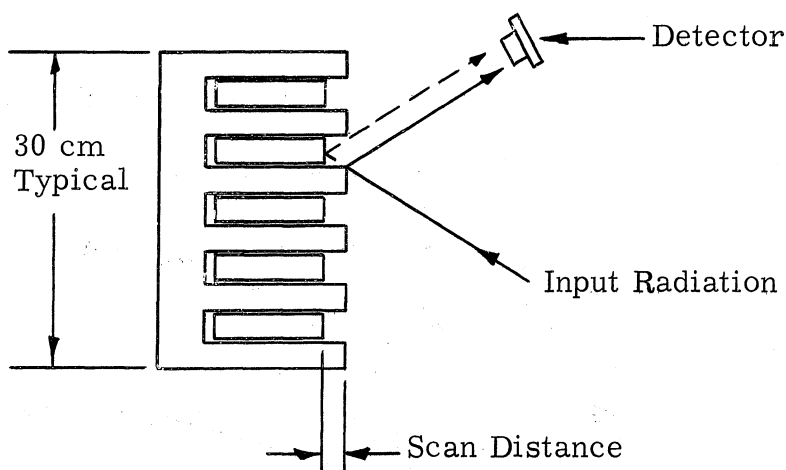


Fig. 20 Lamellar Grating

The beam is split into two components by the grating. There is a physical limitation in the fabrication of the individual grating facets which places a practical limit on the minimum size. The minimum size of the facets restricts the technique to the far infrared. A disadvantage of this technique is that the wavefront is not circularly symmetrical and much of the off-axis radiation is lost. Several instruments of this type have been constructed and are currently being used in the far infrared.

5.5 Variations

The variations noted in this section are those which could be applied to more than one instrument type and are not fundamental in character.

Mirror rotation corrections - The problem of maintaining mirror alignment throughout the full travel of the moving mirror is extremely difficult as the scan distance is increased. For this reason, various techniques to compensate for mirror rotation have been devised. The methods include the replacement of the Michelson mirrors by either a corner reflector¹⁸ or parabolic reflector⁶ (cat's eye) and the folding of the optical paths (see 3.1). All of these techniques lengthen the total optical path which tends to reduce the field of view. In the case of the parabolic cat's eye reflector the energy must also be very well colimated.

Wide angle compensation - It was previously noted that the off-axis rays travel oblique paths through the instrument. As a result, there is a relative displacement of the interfering off-axis rays. The displacement increases as the path difference between the Michelson mirrors increases producing a corresponding decrease in sensitivity.

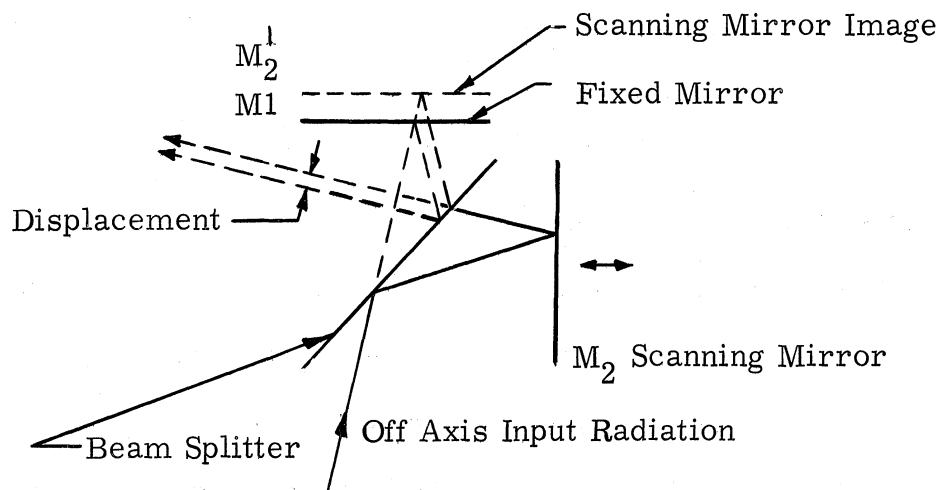


Fig. 21 Off-Axis Ray Displacement

Mertz¹³ proposed compensating for this effect by placing a higher index of refraction material in the scanning mirror optical path. This would completely compensate the instrument at a fixed scan distance. The scanning of such an instrument would be accomplished by making the refracting material wedged shaped and sliding the wedge in front of the mirror.

The construction of a completely compensated interferometer would present many practical problems. However, a specialized working instrument that makes use of this principal has been described by Hilliard and Shepherd.³⁰ Their instrument is constructed for a narrow range of path differences about a fixed central path by using a stationary piece of glass in front of the fixed mirror. The instrument is used to measure the width of a single isolated atomic line.

Digitizing techniques - It was previously noted that most instruments use either Moire or monochromatic fringes as the digitizing reference. In addition to the monochromatic reference it is common practice to insert a

white light fringe signal in the same channel to mark the point of zero retardation. The pulse generated by the white light fringe may be used to initiate the digitizing process.

The most novel digitizing technique is the step recording method. The moving mirror is displaced an integral number of wavelengths of the reference fringe as rapidly as possible. The mirror is stopped at this position and the signal is integrated for a given length of time depending on the intensity of the source before sampling. This technique is used by the Connes in their latest instrument.⁶

6.0 CALIBRATION

The problems associated with the calibration of the interferometer as compared to other spectroscopic devices are not unique. Therefore, the discussion presented here has been deliberately limited.

The final spectral output of the instrument is radiance as a function of wavelength convolved with the instrument function. In order to obtain the final output, a calibration consisting of the measurement of the sensitivity as a function of wavelength with a prior knowledge of the instrument function must be made. The factors to be determined are wavelength accuracy, sensitivity, and the form of the instrument function.

6.1 Wavelength

If the interferometer uses a well defined monochromatic line for the digitizing signal, a wavelength calibration in the ordinary sense is not required. It will be recalled from the theory that

$$\nu' = \nu \left(1 - \frac{v^2}{4\pi} \right) \quad (22)$$

This is the field of view correction which must be made to correct for the variation in the optical path lengths across the field of view. The given relation assumes a well defined field of view which is not always the case. The calibration is a determination of the accuracy of this correction. In the case of the HAEL interferometer the wavelength correction derived from equation (22) is approximately equal to 10^{-3} . Based on the uniformity of field measurements the correction should be accurate to at least 10 percent. Hence, the ultimate wavelength accuracy is one part in 10^{-4} .

The standard calibrating procedure is to measure the position of known lines at both ends of the frequency range. Care must be exercised to completely fill the field of view of the instrument. The ideal source would be a laser to illuminate a diffusing plate which fills the field of view. Such a procedure is usually not possible, and in the infrared it is often more practical to use absorption bands rather than emission lines. In the past we have used plastics such as polystyrene, but we are now using absorption cells containing gas such as carbon dioxide.

6.2 Sensitivity

The sensitivity is a non-linear function of frequency and depends on every part in the optical and electric path from the input radiation to the output signal. The only way to establish the sensitivity function is to use a calibrating source of known intensity. In the infrared region the usual source is a black body of known emissivity and known temperature.

The interferometer developed by the High Altitude Engineering Laboratory has two built-in black bodies operating at both ends of the temperature range. These are used for continuous inflight calibration. The

ultimate RMS noise measurements obtained from this instrument for a single 10 second scan was 0.5 ergs/cm·sec·sr where the maximum signal was 120 ergs/cm·sec·sr.

If black bodies are not available, the problem of making accurate radiance measurements is very difficult since secondary standards are involved.

6.3 Scanning Function

To measure accurately the interferometer scanning function, it would be ideal to have a delta function which could be scanned across the spectrum. If several lasers were available, this would be ideal. Another technique is to use a monochromator, but it is difficult to find a monochromator which will provide a line narrow enough for the purpose.

The technique which we are now developing is to measure the emission from samples of CO₂ and then to compare the measured spectrum with a calculated spectrum convolved with a series of scanning functions. The scanning function is deduced from the best match.

7.0 SUMMARY

Fourier transform spectroscopy is an extremely powerful spectroscopic technique, and because of its inherently superior light gathering ability, it will find many applications. However, the development of the technique has been rather slow. There are several reasons for this, but the most important has been the long computer turn-around time measured in days rather than in minutes.

The computer and computational bottlenecks to the development of

the method seem to be on the verge of being broken with the advance in computer technology and the introduction of more powerful computational techniques. Therefore, we are looking forward to the rapid development of the technique in the near future and its application to many spectroscopic problems.

REFERENCES

1. Mertz, L. (1965), Transformations in Optics, John Wiley & Sons, New York.
2. Loewenstein, E. V. (1966), Applied Optics 5, 845.
3. Bell, E. E. (1966), Infrared Physics 6, 57.
4. Forman, M. L., Steel, W. H., and Vanasse, G. A., Non-linear Phase Connections of Interferograms Obtained in Fourier Spectroscopy, AFCRL-65-518.
5. Connes, J. (1961), Rev. Optique 40, 45, 116, 171, 231, an English translation is available as a Navy publication, NAVWEPS report no. 8099, NOTSTP 3157, published by the U. S. Naval Ordnance Test Station, China Lake, California.
6. Connes, J. & P. (1966), J. Opt. Soc. Am. 56, 896.
7. Dowling, J. M. (1966), J. Opt. Soc. Am., Annual Meeting, FC 1.
8. Chaney, L. W., Drayson, S. R., and Young, C. (Feb. 1967), Applied Optics 6.
9. Fellbett, P. B. (1958), Thesis, University of Cambridge, 1951: J. Phys. Radium 19, 187.
10. Jacquinet, P. (1958), J. Phys. Radium 19, 223: Reports on Progress in Physics 23, 267, (1960).
11. Connes, P. (1956), Rev. Optique 35, 37.
12. Gebbie, H. A., Vanasse, G. A., and Strong, J. (1956), J. Opt. Soc. Am. 46, 377.
13. Mertz, L. (1959), I. C. O., Stockholm, Hetrodyne Interference Spectroscopy.
14. Strong, J. and Vanasse, G. A. (1959), J. Opt. Soc. Am. 49, 844.
15. Mellon Institute Symposium on Far Infrared Transpose Spectroscopy (1965), Pittsburgh, 10-11 June 1965, reported in Applied Optics 4, 1374, (1965).

16. Chaney, L. W. (1964), Earth Radiation Measurements by Interferometer from a High Altitude Balloon. Proceedings of the Third Symposium on Remote Sensing of the Environment, Ann Arbor, Michigan.
17. Gush, H. P. and Buijs, H. L. (1964), *Cam. S. Phys.* 42, 1037.
18. Willson, R. C., The Theory, Design and Development of an Interferometer Spectrometer, University of Colorado Science Report No. 1, Project 8627.
19. Pritchard, J. L., Sakai, H., Steel, W. H., and Vanasse, G. A. (1966), Mobius Band Interferometer and Its Application to Fourier Spectroscopy, Collogue Sur les Methods de Spectroscopie Instrumentale, Bellevue France.
20. Surh, M. T. (1966), *Applied Optics* 5, 880.
21. Forman, M. L., Steel, W. H., and Vanasse, G. A. (1966), *J. Opt. Soc. Am.* 56, 59.
22. Gibbs, J. E. and Gebbie, H. A. (1965), *Infrared Physics* 5, 187.
23. Billings, B. (Feb. 1963), Research in Infrared Interferometry and Optical Masers, Baird Atomic, Inc., Final Report AF 19(604)2264.
24. Cooley, J. W. and Tukey, J. W. (1965), *Math Computations* 19, 296.
25. Gebbie, H. A., Habell, K. J., and Middleton, S. P. (1962), Proc. of the Conf. on Opt. Inst. and Tech. (Chapman and Hill, Ltd., London 63).
26. Bosomworth, D. R. and Gush, H. P. (1965), *Cam. J. Phys.* 43, 729.
27. Wheeler, R. E. and Hill, J. C. (1966), *J. Opt. Soc. Am.* 56, 657.
28. Genzel, L. and Weher, R. (1958), *Z. Angew. Phys.* 10, 127 (1958): 10, 195.
29. Richards, P. L. (1964), *J. Opt. Soc. Am.* 54, 1474.
30. Hilliard, R. L. and Shepherd, G. G. (1966), 56, 362.
31. Hanel, R. A. and Chaney, L. W. (July 1964 and March 1965), The Infrared Interferometer Spectrometer Experiment (IRIS), Goddard Space Flight Center Reports X-650-64-204 and X-650-65-75.



3 9015 02829 9603

THE UNIVERSITY OF MICHIGAN

DATE DUE

11/6 16:04